

Analysis of Fixed Flight Path Angle Descents for the Efficient Descent Advisor

Minghong G. Wu

University of California, Santa Cruz, Moffett Field, California, 94035-1000

Steven M. Green

NASA Ames Research Center, Moffett Field, California, 94035-1000

NASA STI Program ... in Profile

Since its founding, NASA has been dedicated to the advancement of aeronautics and space science. The NASA scientific and technical information (STI) program plays a key part in helping NASA maintain this important role.

The NASA STI Program operates under the auspices of the Agency Chief Information Officer. It collects, organizes, provides for archiving, and disseminates NASA's STI. The NASA STI Program provides access to the NASA Aeronautics and Space Database and its public interface, the NASA Technical Report Server, thus providing one of the largest collection of aeronautical and space science STI in the world. Results are published in both non-NASA channels and by NASA in the NASA STI Report Series, which includes the following report types:

- **TECHNICAL PUBLICATION.** Reports of completed research or a major significant phase of research that present the results of NASA programs and include extensive data or theoretical analysis. Includes compilations of significant scientific and technical data and information deemed to be of continuing reference value. NASA counterpart of peer-reviewed formal professional papers, but having less stringent limitations on manuscript length and extent of graphic presentations.
- **TECHNICAL MEMORANDUM.** Scientific and technical findings that are preliminary or of specialized interest, e.g., quick release reports, working papers, and bibliographies that contain minimal annotation. Does not contain extensive analysis.
- **CONTRACTOR REPORT.** Scientific and technical findings by NASA-sponsored contractors and grantees.

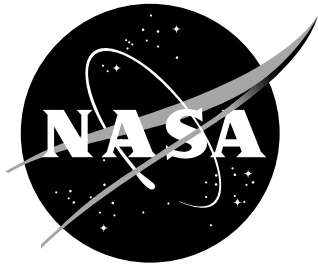
- **CONFERENCE PUBLICATION.** Collected papers from scientific and technical conferences, symposia, seminars, or other meetings sponsored or co-sponsored by NASA.
- **SPECIAL PUBLICATION.** Scientific, technical, or historical information from NASA programs, projects, and missions, often concerned with subjects having substantial public interest.
- **TECHNICAL TRANSLATION.** English-language translations of foreign scientific and technical material pertinent to NASA's mission.

Specialized services also include creating custom thesauri, building customized databases, and organizing and publishing research results.

For more information about the NASA STI Program, see the following:

- Access the NASA STI program home page at [*http://www.sti.nasa.gov*](http://www.sti.nasa.gov)
- E-mail your question via the Internet to [*help@sti.nasa.gov*](mailto:help@sti.nasa.gov)
- Fax your question to the NASA STI Help Desk at 443-757-5803
- Phone the NASA STI Help Desk at 443-757-5802
- Write to:
NASA STI Help Desk
NASA Center for AeroSpace Information
7115 Standard Drive
Hanover, MD 21076-1320

NASA/TM-2011-215992



Analysis of Fixed Flight Path Angle Descents for the Efficient Descent Advisor

Minghong G. Wu

University of California, Santa Cruz, Moffett Field, California, 94035-1000

Steven M. Green

NASA Ames Research Center, Moffett Field, California, 94035-1000

National Aeronautics and
Space Administration

Ames Research Center
Moffett Field, California, 94035-1000

November 2011

The use of trademarks or names of manufacturers in this report is for accurate reporting and does not constitute an official endorsement, either expressed or implied, of such products or manufacturers by the National Aeronautics and Space Administration.

Available from:

NASA Center for AeroSpace Information
7115 Standard Drive
Hanover, MD 21076-1320
443-757-5802

Abstract

Sensitivity analysis of fixed-flight-path-angle descents for the Efficient Descent Advisor is performed, probing various angles, winds, and times to fly, and using a high fidelity aircraft performance model. Three strategies for choosing fixed flight path angle descents are proposed and analyzed under realistic test conditions. Trade-offs between fuel burn and speed brake usage in the choice of the flight path angle are investigated and discussed. Comparison of these three strategies shows less than 20 lbs of fuel burn difference when full speed brake usage is allowed in the predicted trajectory. Two of the strategies, using a universal flight path angle and using a flight path angle as a function of the descent calibrated airspeed, are more sensitive to speed brake constraints and can have up to 112 lbs and 90 lbs of fuel burn penalty when speed brake usage is disallowed. The third strategy, the custom flight path angle, demonstrates the most fuel-efficiency and saves more fuel than the idle-thrust descent by an average of 41 lbs.

Nomenclature

γ_i	Inertial flight path angle
BJ	Business jet
CAS	Calibrated airspeed
CDA	Continuous Descent Approach
EDA	Efficient Descent Advisor
ETA	Estimated time of arrival
FMS	Flight Management Systems
FPA	Flight path angle
HITL	Human-in-the-loop
ILS	Instrument Landing System
RJ	Regional jet
STA	Scheduled time of arrival
TAS	True airspeed
TMA	Traffic Management Advisor
VNAV	Vertical Navigation

1 Introduction

The Efficient Descent Advisor (EDA) [1–5] is being developed by NASA as a key capability for the Next-Generation Air Transportation System (NextGen) [6–8]. A trajectory-based decision-support tool intended for use by controllers working in FAA en-route air traffic control facilities, EDA is capable of generating dynamic Continuous Descent Approach (CDA) trajectories for arrivals transitioning from en-route to terminal airspace. The advisories generated by EDA take into account airspace restrictions, aircraft performance, atmospheric conditions, conflict avoidance, and the required time of arrival satisfying the time-based metering schedule computed by the Traffic

Management Advisor (TMA) [9]. TMA specifies at which time each airplane is required to cross a meter fix located at the Terminal Radar Approach Control Facilities (TRACON) boundary for optimal arrival throughput.

A series of human-in-the-loop (HITL) simulations were conducted in 2009 through 2011 for testing the concept of EDA [1,2]. These simulations focused on aircraft equipped with performance-based flight management systems (FMS). With a descent speed given by the EDA advisory, the vertical navigation (VNAV) of a performance-based FMS generates an idle- or near-idle thrust descent trajectory for that descent speed. However, these HITL simulations did not incorporate fixed flight path angle (FPA) descent procedures employed by regional (RJ) and business jet (BJ) types; these represent about one-third of aircraft operations today. There are no standards for such procedures to define the FPA to be flown, and actual operations can vary greatly.

Any practical EDA clearances for BJs or RJs must allow for fixed-FPA descent procedures. Limited analysis of fixed-FPA descents exists in the literature [10–12], and the sensitivity of feasible, fuel-efficient FPAs to varying environmental conditions is far from understood. This work attempts to obtain insight into fixed-FPA descents and to design practical fixed-FPA descent procedures. It investigates the effect of FPA on the fuel burn of the trajectory, analyzes the sensitivity of the fuel-optimal FPA to flight conditions, and proposes three FPA selection strategies. Three different speed brake conditions are imposed on each strategy to model different levels of robustness requirements. Monte Carlo simulations of test conditions are performed to optimize and evaluate these selection strategies.

This paper is organized as follows: Section 2 gives background information on fixed-FPA descents, reviewing past work and discussing factors to consider in the design of descent procedures. Section 3 describes modeling schemes and methods for solving the intrinsic meet-time problem in EDA. Section 4 examines in depth a representative EDA test condition and investigates the sensitivity of the fuel burn and speed brake usage to the FPA. Section 4 further studies the sensitivity of the fuel-optimal FPA to the variation of wind and target time. Section 5 presents three FPA selection strategies, three speed brake conditions, and discusses the sampling of realistic test conditions defined by wind, weight, and target time. Results of comparison of the three FPA selection strategies are also presented in Section 5. Section 6 discusses in more detail a few related observations of the results given in Sections 4 and 5. Finally, we conclude in Section 7 and discuss future work to be done.

2 Background

Larger jets equipped with performance-based flight management systems (FMS) are capable of generating and flying idle-thrust descents. Idle-thrust descents are intrinsically sensitive to the aircraft’s performance parameters, the descent speed profile, and atmospheric conditions [13,14], and predictions of the idle-thrust descents have proved challenging [15,16]. Fixed-FPA descents, on the other hand, have the potential of being more predictable by the ground automation tools. Most BJs and RJs are equipped with a kinematic FMS that can provide guidance for fixed-FPA descents. This type of FMS, however, cannot guide idle-thrust descents. Large commercial jets equipped with a performance-based FMS, on the contrary, do not have built-in capabilities for

executing fixed-FPA descents. Nonetheless, potential procedures to execute fixed-FPA descents using performance-based FMS have been suggested [10].

Field tests for fixed-FPA procedures were conducted at Denver Center in 2010 using the FAA Global 5000 test aircraft and participating Skywest regional flights to understand the feasibility of pilot/controller procedures and determine trajectory prediction accuracies. Pilots determined the FPA to fly using a published function of the descent calibrated airspeed (CAS). However, no attempt was made to optimize the function for the tests.

Many factors should be considered for the design of fixed-FPA descent procedures, but robustness, i.e., the ability to consistently execute a continuous descent, out-weighs all other factors. Steep descent angles will not be flyable under certain combinations of wind, speed, and weight conditions. Even if a steep descent is achievable with the use of speed brakes, many pilots are reluctant, if not unwilling, to use them because of noise and ride discomfort. On the other hand, shallow descent angles burn more fuel, increasing cost and environmental impact. Pilot procedures, airspace restrictions, aircraft equipage, and traffic separation should also be taken into account. A fixed-FPA descent procedure must also provide a way to define the FPA for both controllers and pilots.

Analysis of various descent strategies has been done in a pioneering work [11,12] by Izumi et al. at Boeing. They compared idle-thrust descent, fixed-FPA descent, and fuel-optimal descent strategies in a metering environment in terms of their fuel burn and the mixed traffic throughput they achieve. Although constant time to fly is assumed, their work did not explore the variation of wind or the FPA. Tong et al. have considered the design of fixed-FPA descent strategies within the 3D-PAM concept [10], which is enabled by EDA capabilities. Their work touched upon the variation of FPA on fuel burn, but the trajectories were compared on a basis of identical descent speeds instead of identical times to fly. This work will explore the variation of wind, weight, and time-to-fly, quantifying their effect on the fuel-optimal FPA.

Idle-thrust descents have been frequently referred to as fuel-optimal descents in the literature [10, 17,18]. Although idle thrust is fuel-optimal for the descent segment alone, it does not necessarily achieve fuel-optimal trajectories overall. Izumi et al. [12] compared computed fuel-optimal trajectories using the singular perturbation theory. They made a clear distinction between a fuel-optimal trajectory and an idle-thrust trajectory. The fuel-optimal trajectory for B747 showed less fuel burn and a much earlier top-of-descent than the idle-thrust trajectory. In this work we compare the fuel-optimal fixed-FPA descent to the corresponding idle-thrust descent under the same test condition in the context of a constant-time-to-fly problem. These comparisons will show that a fixed-FPA descent can actually burn less fuel than an idle-thrust descent.

3 Modeling Schemes and Methods

Consider a typical arrival flight in en-route airspace that has just entered the TMA freeze horizon, where the TMA schedules and freezes the flight's scheduled time of arrival (STA) at the meter fix [19]. In heavy traffic conditions, TMA imposes flow management by ensuring sufficient time spacing between aircraft at the metering fix. In such conditions the STA usually delays the aircraft with respect to its predicted nominal arrival time, denoted as the estimated time of arrival (ETA). EDA attempts to absorb the time delay by computing a speed advisory that meets the STA by

reducing the cruise and descent speeds of the aircraft’s trajectory. If speed changes are not enough to absorb the delay time, EDA stretches the horizontal route in addition to reducing speeds. During the HITL simulations altitude changes are occasionally issued in combination with speed changes to avoid conflicts [2]. In this work, we constrain the solution space to those aircraft requiring speed changes only. While the analysis in this work is based on a simple, direct route to the meter fix, it can be readily extended to general horizontal routes.

3.1 Vertical Profile Modeling

The model of the vertical profile for an arrival flight in the en-route airspace, when described in terms of the altitude’s status, consists of a cruise segment, a descent segment and, if necessary, a level deceleration segment to the meter fix. Taking into account the distinct control variables applied during the flight, we further break down the cruise and descent segments to a combination of some or all of the following five segment types:

1. An acceleration/deceleration cruise segment at the cruise altitude
2. A constant airspeed cruise segment at the cruise altitude
3. A constant Mach descent segment
4. A constant calibrated airspeed (CAS) descent segment
5. A deceleration level segment at the meter-fix crossing altitude.

Figure 1 demonstrates a general vertical profile that has all the five segment types. Note that segment 1 exists only if the cruise speed in the advisory is different than the aircraft’s current speed. Segment 3 exists only if the descent CAS is greater than the cruise CAS in the advisory. Segment 5 exists only if the descent CAS in the advisory is greater than the meter-fix crossing speed.

For this work each segment is modeled by fixing two control parameters. For a cruise segment the model fixes a parameter, which is engine control or an airspeed, and sets the FPA to zero. For the constant speed descent segments, the model fixes an airspeed in Mach or CAS and fixes another parameter, which can be engine control or FPA.

3.2 Trajectory Synthesis

For the purpose of this study, the Center-TRACON Automation System (CTAS) Trajectory Synthesizer (TS) [20–22] is used to simulate the trajectories to be analyzed. TS takes as its input a flight’s current position and velocity, flight plan, airspace restrictions, a model of pilot’s intent, wind and temperature aloft, and aircraft performance model. The output is a trajectory defined by the aircraft’s 3-D position and velocity as a function of time along with computed forces and fuel burn.

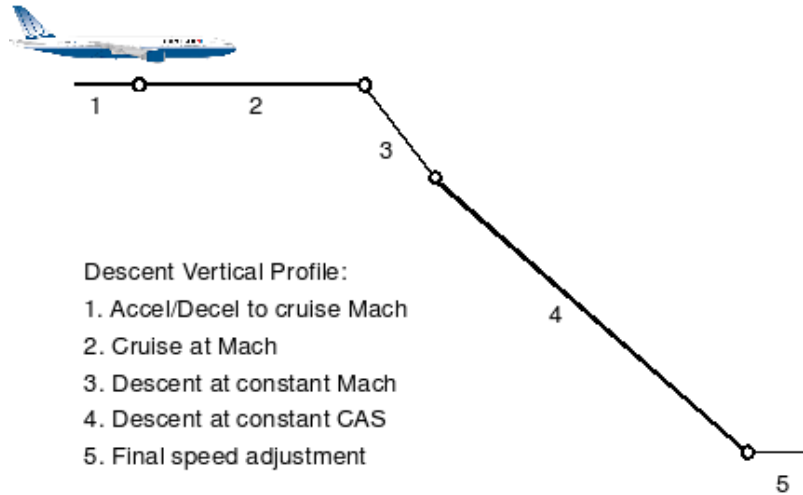


Figure 1. A general vertical profile that contains five segment types.

TS uses an aircraft performance model database that has been validated and improved by various research projects [23]. We selected a model representative of a mid-size, narrow-body, twin-engine jet airliner with a typical descent weight of approximately 170,000 lbs. Although this model represents an aircraft larger than RJs and BJs, it has been validated against other tools such as Boeing’s INFLT and should provide high-fidelity results. The minimum cruise and descent CAS speeds for delay advisories are set at 250 knots and the maximum cruise mach and descent CAS are set at 0.84 and 350 knots, respectively.

The maximum drag that can incur as a result of speed brake deployment, defined as the speed brake capacity, is modeled as a maximum speed brake drag coefficient. The chosen aircraft model in TS did not have parameters for speed brake. We asked a few pilots to estimate the maximum speed reduction the full speed brake deployment can effect at a few typical descent conditions. Their estimates of speed reductions were used to derive an empirical maximum speed brake drag coefficient.

3.3 Initial and Environmental Conditions

Throughout the rest of the modeling work a hypothetical flight is heading toward the meter fix from a distance of 150 nautical miles (nmi), a typical distance for the TMA freeze horizon [19]. The aircraft is initially level at 35,000 ft and its initial airspeed is 0.80 Mach, typical for aircraft of this type. The meter-fix crossing restrictions are an altitude of 10,000 ft and a CAS of 250 knots or less.

Wind is modeled as a function linear in altitude that has intercept zero at sea level. The direction of wind is the same at all altitudes and has only horizontal components. This linear approximation is reasonable within the range of altitude of interest but becomes unrealistic above 35,000 ft or below 6,000 ft [24]. Standard atmospheric conditions are assumed for temperature and pressure as functions of altitude.

The target time is chosen within the time range achievable by speed changes of the aircraft. Idle thrust descents were used in defining this achievable time range. We neglect the slight expansion of this achievable time range that fixed FPA descents can do. This ensures that the comparison of fixed-FPA descents to the idle-thrust descents can be made at any test condition.

3.4 Meet-Time Analysis

A meet-time analysis computes a family of trajectories of varying FPAs for a specific time-to-fly to the meter fix. Both FPA and the speed profile may be varied in the process of computing a trajectory to meet the target arrival time at the meter fix. Suppose we fix the FPA. Iterating the speeds for a trajectory that meets the target time, we could have varied the cruise and descent speeds independently. This simplistic approach can produce operationally impractical speed changes. One extreme example is a speed-up in cruise followed by a speed-down in descent, while the same target time can be achieved by maintaining the current CAS in cruise and descent. Taking into account practical issues, EDA supports three distinct speed modes, referred to as Descent-Only, Cruise-Only, and Cruise-Equals-Descent [3]. The Cruise-Equals-Descent mode can absorb the most delay and therefore is used in this work.

The Cruise-Equals-Descent mode attempts to identify solutions where the cruise CAS and descent CAS are adjusted to minimize the difference between the two speeds. Some operational considerations are accommodated in this mode and the resulting cruise and descent speeds are not always equal. For example, this speed mode attempts to maintain the aircraft’s current airspeed and use the nominal descent speed. If the target time can be achieved by just varying one of the two, EDA does so without enforcing that the cruise and descent speeds be equal. Further modeling details can be found in [3].

Although both the FPA and the speeds can be computationally represented as continuous parameters, we have restricted the FPAs to multiples of 0.1° , using negative values to represent descents. The choice of one decimal place for the FPA matches the precision of the FPAs published to the pilots in the flight test conducted at Denver Center in 2010. It also matches the precision in typical flight deck automation. Speeds are solved for the meet-time problem as precisely as the computer’s precision allows for this work, although the actual EDA clearance gives the speeds as multiples of knots. In the following sections the symbol γ_i represents the FPA value of a descent.

Spanning FPAs from $\gamma_i = -1.8^\circ$ to $\gamma_i = -6.0^\circ$, the meet-time analysis iterates in the Cruise-Equals-Descent speed mode to obtain the correct speed profile for that FPA and the STA. The minimum cruise and descent speeds restrict the solution space on the slow end where delays are large. The maximum cruise and descent speeds limit the solution space where the STA is earlier than the ETA. Speed brake capacity defines the steepest FPA for many conditions studied. The path distance may limit the shallower descent if its range is too short to accommodate the speed changes and the descent segment. For the choice of 150 nmi, initial Mach of 0.80, and modeled winds, we find that the shallowest FPA of -1.8° used in the study was always achievable.

4 Sensitivity Analysis

Fuel burn and speed brake usage are two major factors to consider in the efficient and robust choice of FPA. How sensitive are these factors to the selection of an FPA in a typical test condition? Does a fuel-optimal fixed-FPA trajectory require speed brakes? Is it always less fuel-efficient than an idle-thrust descent trajectory? To shed some light on these questions, Section 4.1 picks a representative test condition and analyzes a family of fixed-FPA trajectories in terms of their fuel burn, speed brake usage, and descent speed profiles.

Wind has strong influence on the vertical profile, and Section 4.2 studies wind effects on the variation of idle-thrust and fuel-optimal fixed-FPA trajectories. The effect of the target time on the variation of the fuel-optimal FPA is also investigated in Section 4.2.

4.1 Sensitivity of Fuel Burn and Speed Brake to FPA

A meet-time analysis at standard atmospheric conditions without wind was performed. The time to fly was selected to be 1,311 seconds, 40 seconds more than the nominal time the aircraft would have flown based on the nominal trajectory with the nominal speed profile of 0.8 Mach in cruise and 0.8/290 knots in descent.

Figure 2 depicts the fuel burn of trajectories flying with different FPAs. The fuel-optimal FPA is approximately $\gamma_i = -2.75^\circ$ for this test condition. Analysis of the trajectories indicates that those with FPAs steeper than $\gamma_i = -2.7^\circ$ would require speed brake usage, and trajectories with FPAs steeper than $\gamma_i = -3.6^\circ$ exceed the speed brake capacity during part or all of the descent. Even with full speed brake deployment the aircraft is unable to descend steeper than $\gamma_i = -3.6^\circ$. Note that the fuel burn of trajectories between $\gamma_i = -2.6^\circ$ and $\gamma_i = -2.9^\circ$ is less than the fuel burn of the corresponding idle-thrust descent, whose fuel burn is represented by the gray horizontal line on Figure 2. This is not specific to this test condition as later analysis will show that fixed-FPA descents can be more fuel-efficient than idle-thrust descents on average.

Figure 3 shows the corresponding altitude profiles with different descent FPAs. The idle-thrust descent profile is close to the $\gamma_i = -3.0^\circ$ fixed-FPA descent. The idle-thrust descent operates on the boundary of the speed brake “region,” and any descents steeper than the idle-thrust descent are expected to require speed brake usage. However, the $\gamma_i = -2.8^\circ$ descent requires speed brake usage even though its descent is shallower than the idle-thrust descent. This counter-intuitive result is explained later in Figure 5 after we examine the speed profile of each trajectory.

Figure 4 shows the CAS profile for each trajectory. Recall that the Cruise-Equals-Descent speed mode in EDA is applied in determining the cruise and descent CAS values for each trajectory. In general, shallower descents require higher cruise and/or descent CAS values to meet the same time to compensate for the lower true airspeed (TAS) associated with the CAS at lower altitudes. The shallowest fixed-FPA descent shown in Figure 4, with the FPA $\gamma_i = -2.0^\circ$, requires a cruise at 0.84 Mach (287 knots CAS) and a descent at 0.84 Mach and 291 knots CAS. The vertical profile of this trajectory contains the five distinct segments described in section 3.1: an initial acceleration in cruise, a constant speed in cruise, a constant mach descent, a constant CAS descent, and a deceleration level. The trajectory with $\gamma_i = -2.2^\circ$ has a longer cruise portion of flight and thus

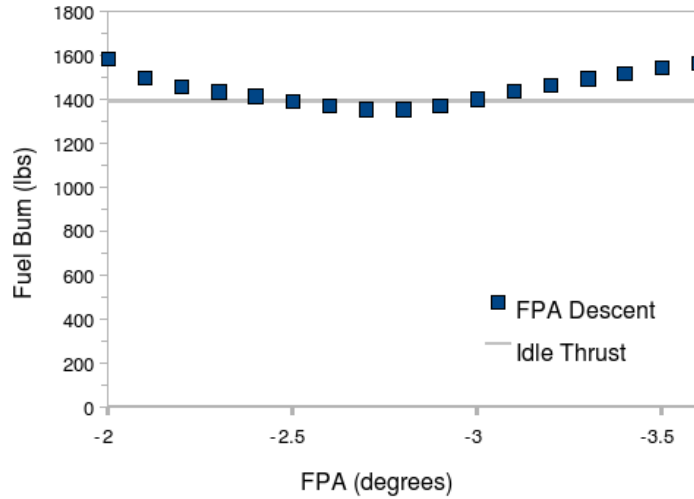


Figure 2. Fuel burn variation with flight path angle. The time to fly is 1,311 seconds.

requires lower speeds to meet time, 273 knots CAS for cruise and 290 knots CAS for descent. The decrease in speeds continues as the descent FPA gets steeper. Note that the cruise CAS does not equal descent CAS until the FPA becomes steeper than $\gamma_i = -3.0^\circ$. This is because preference is given to the current cruise speed and the preferred descent speed in the Cruise-Equals-Descent speed mode. If only one change of the speeds from these two preferred values is enough to meet the time, EDA fixes the other at the preferred value.

Figure 5 provides insight to the need for speed brakes during the descent. The vertical axis represents one of two events that do not happen simultaneously in the modeling scheme: the additional thrust above idle or speed-brake usage. Its value is meaningful only for the descent segments of the trajectory. Positive values represent the excess thrust required above idle to maintain the aircraft on the FPA at the designated speed. Negative values represent the drag required by the speed brake to keep the aircraft on the FPA at the designated speed. For shallow descents such as $\gamma_i = -2.0^\circ$, the whole descent requires excess thrust, thus consuming more fuel during descent. The trajectory with $\gamma_i = -2.8^\circ$ uses speed brake at a path distance of -84 nmi and needs excess thrust above idle before and after. At -84 nmi the trajectory is at 34,000 ft altitude. This need for speed brake occurs right below the Mach-CAS transition. Above the Mach-CAS transition altitude, the local FPA flown by an idle-thrust descent at 0.8 Mach is much steeper than $\gamma_i = -2.8^\circ$. Therefore, thrust is required in the constant-Mach descent segment to maintain $\gamma_i = -2.8^\circ$. Upon transition to a constant CAS segment, the FPA flown by an idle thrust descent at 278 knots CAS becomes slightly shallower than $\gamma_i = -2.8^\circ$. Therefore, speed brake usage is required during this part of the descent. As the aircraft descends to lower altitudes, the local FPA of the idle thrust descent gradually becomes steeper, crossing over the angle of -2.8° again. Therefore the aircraft transitions from speed brake usage to excess thrust above idle. This double crossover is observed for the $\gamma_i = -3.0^\circ$ trajectory too. For trajectories steeper than -3.2° , the power is on idle throughout the descent, with speed brake deployed for the entire descent. Trajectories steeper than -3.6° require more speed brake than available.

Figure 6 shows the rate of fuel burn as a function of time. The area under a curve equates to the

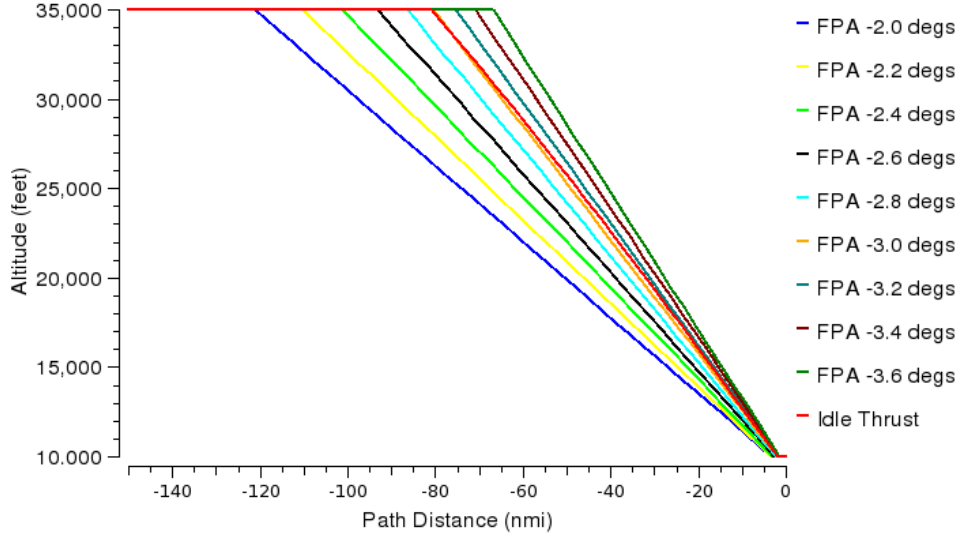


Figure 3. Altitude along the path distance. The time to fly is 1,311 seconds.

total fuel burn for the entire flight. Note, the idle-thrust fuel burn curve is largely coincident with the $\gamma_i = -3.0^\circ$ fixed-FPA descent curve. The $\gamma_i = -2.0^\circ$ trajectory has an acceleration segment in cruise from 0.80 Mach to 0.84 Mach characterized by a burn rate that well exceeds the nominal rate in cruise. This acceleration segment is followed by a constant-mach cruise segment with a fuel burn rate of about 9,500 lbs/hr. The top of descent for the $\gamma_i = -2.0^\circ$ trajectory happens at 215 seconds when the flight transitions to a constant-Mach/constant-FPA descent segment that lasts for 18 seconds. This segment has an average fuel burn rate of about 5,300 lbs/hr. The flight then transitions to a long constant-CAS/constant-FPA descent segment at 233 seconds until it reaches the bottom of descent at about 1,272 seconds. In all trajectories this segment has a fuel burn rate that slowly increases as the flight descends. The flight then levels off and decelerates to 250 knots at the meter fix at 1,311 seconds. This final decelerating segment has an average low fuel burn rate of about 1,400 lbs/hr. Similar segments are observed for the $\gamma_i = -2.2^\circ$ trajectory. The trajectories with γ_i values of -2.4° , -2.6° , -2.8° , and -3.0° do not have an accelerating cruise segment at the beginning. Instead, they cruise at the initial Mach to their top of descent points. The trajectories with γ_i values of -3.2° , -3.4° , and -3.6° have deceleration cruise segments to lower cruise speed. They do not have a constant Mach descent segment because they cruise and descend at the same CAS.

Of the trajectories shown in Figure 6, the $\gamma_i = -2.8^\circ$ descent consumes 1,351 lbs of fuel, 38 lbs less than the value of 1,389 lbs for the idle-thrust descent. Both trajectories have the same fuel burn rate in cruise due to their identical cruise speed. The $\gamma_i = -2.8^\circ$ fixed-FPA trajectory starts descending 45 seconds earlier than the idle-thrust trajectory, and thus consumes less fuel in the cruise segment. However in the descent segment, the $\gamma_i = -2.8^\circ$ trajectory consumes more fuel than the idle-thrust trajectory, especially near the bottom of descent. Nonetheless, the fuel benefit gained by the $\gamma_i = -2.8^\circ$ trajectory in the cruise segment exceeds the fuel burn penalty in the descent, resulting in an overall fuel burn advantage of 38 lbs.

The same observation is made on Figure 7 regarding the fuel burn trade-offs between cruise and

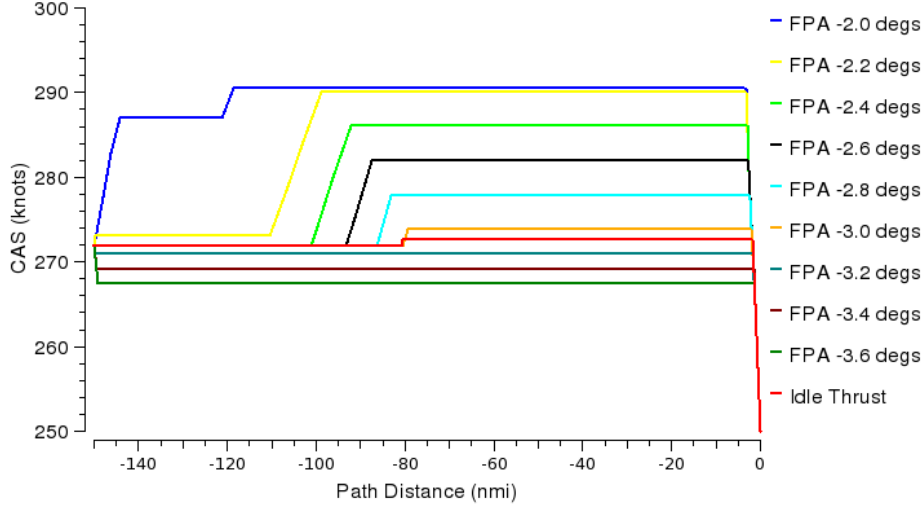


Figure 4. Calibrated airspeed along the path distance. The time to fly is 1,311 seconds.

descent. The fuel burn values at the end of the curves correspond to the fuel burn values in Figure 2. The local slope of each curve represents the rate of fuel burn plotted in Figure 6. The trajectory with the shallowest descent, $\gamma_i = -2.0^\circ$, has the most overall fuel burn due to its high cruise speed and long, less fuel-efficient descent phase. The most fuel-efficient fixed-FPA trajectories are those near $\gamma_i = -2.8^\circ$. When compared with the idle-thrust trajectory, the $\gamma_i = -2.8^\circ$ trajectory gains an advantage in fuel with its earlier descent. The difference between idle-thrust and the $\gamma_i = -2.8^\circ$ trajectory diminishes in the descent phase, but in the end the $\gamma_i = -2.8^\circ$ trajectory burns 38 lbs less. The trajectories with FPA steeper than $\gamma_i = -3.0^\circ$ all have very fuel-efficient descent phases, but they spend more time in cruise and therefore burn too much fuel in their cruise phase, resulting in an overall fuel burn penalty.

4.2 Sensitivity of FPA to Wind and Target Time

Three representative wind conditions, no wind, strong head wind, and strong tail wind, are applied to the analysis of meet-time trajectories. The slope of the wind function is chosen so that the wind magnitude at 35,000 ft is 100 knots for both head wind and tail wind conditions. This magnitude of wind is strong but realistic.

The variation of the fuel-optimal FPA due to typical target times is also probed. The three target-time conditions are fast time, nominal time, and slow time. The nominal time is defined as the time flown by the aircraft to the meter fix under the wind condition considered, using a speed of 0.8 Mach in cruise and 290 knots CAS in descent. For this specific comparison, the fast time is defined as 90 seconds earlier, while the slow time is defined as 120 seconds later than the nominal time. The time intervals are selected so that they are far enough from the nominal time and still within the time range achievable by speed maneuvers.

Figure 8 shows the fuel-optimal FPA resulting from the three wind conditions and three target time conditions. As a comparison the effective FPA of the idle-thrust trajectory is computed for

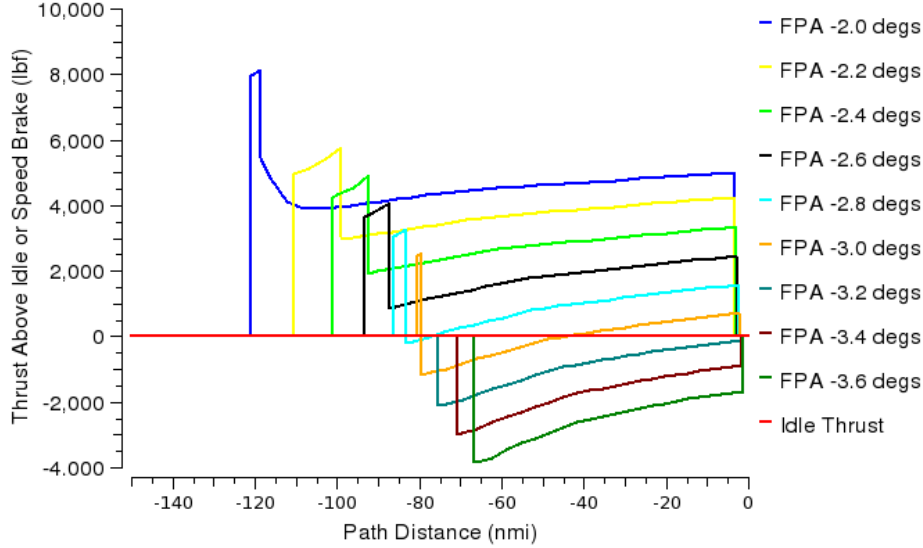


Figure 5. Power above idle or speed brake usage along the descent. The time to fly is 1,311 seconds.

each test condition. The effective FPA of an idle-thrust descent is defined as the angle between the level flight and the line connecting the top-of-descent point in the space with the bottom-of-descent point in the space. As expected, the idle-thrust descent is steeper in the head-wind and shallower in the tail-wind. The idle-thrust descent is steeper for higher descent speeds (fast) and shallower for lower descent speeds (slow). The fuel-optimal FPA also shows similar trends, steeper in a head wind or for faster times and shallower in a tail wind or for slower times. One exception to these trends is the value at -1.8° , denoted by an orange square at the bottom, which we discuss in the next paragraph. Aside from this anomaly, the other fuel-optimal FPAs display less variation over the wind change when compared with the effective FPAs for idle-thrust. For example, the fuel-optimal FPA for nominal time varies from -3.2° in the head-wind to -2.3° in the tail-wind, while the effective FPA of the idle-thrust descent for nominal time varies from -4.19° in the head-wind to -2.58° in the tail-wind, as shown in the diamonds of Figure 8.

The exception for fuel-optimal FPA into a head wind with fast time is further investigated. At the test condition, the fuel burn continues to decrease as the FPA becomes shallower. In fact, the value of -1.8° shown in Figure 8 at this test condition is the shallowest FPA computed in this program. The program may find even shallower trajectories until the cruise segment becomes too short for the acceleration to finish. A closer look at the trajectories at this test conditions reveals that most of these shallow trajectories cruise at the highest cruise speed of 0.84 Mach. This high cruise speed is required to meet the time in the strong head wind. The fuel-burn rate at this cruise speed is about 9,500 lbs/hr. Such a high cruise fuel burn rate would tip the trade-off between cruise and descent and favors early descent for the reduction of the overall fuel burn.

Figure 9 shows the fuel burn of fixed-FPA trajectories as a function of time to fly. The time-to-fly is denoted as Δt in the legend. No wind is applied in these test conditions. The symbols on the curves highlight the trajectories that do not require speed brake usage. The FPA for the steepest speed-brake-free trajectory ranges from -3.5° for a fast time of 1,171 seconds to -2.5° for a slow time of 1,416 seconds. On the fast end of the time range shown at the top with $\Delta t = 1,171$ seconds,

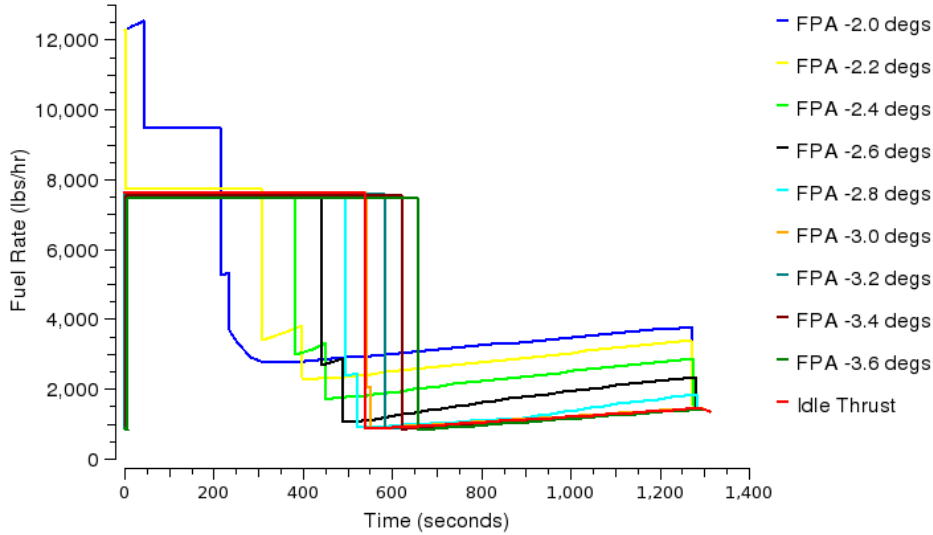


Figure 6. Fuel rate for different FPAs as a function of time. The total path distance is 150 nmi.

shallow descents are bounded by maximum cruise and descent speeds, causing no trajectories to be found for FPA shallower than -2.6° . On the slow end of the time range with $\Delta t = 1,416$ seconds, steep descents are bounded by minimum cruise and descent speeds, causing no trajectories to be found for FPA steeper than -2.9° . In between the ends, the speed brake capacity also bounds the steepest descent a trajectory can have, e.g., $\gamma_i = -3.8$ is the steepest trajectory for a time to fly of 1,271 seconds.

The variation in fuel burn with FPA has an interesting change of slope for $\Delta t = 1,271$ seconds and $\Delta t = 1,281$ seconds near the FPA of -2.9° . The rapid change of overall fuel burn is mostly due to change of cruise speed. For example, in the curve for $\Delta t = 1,271$ seconds the cruise speed changes from 0.839 Mach at -2.6° to 0.815 Mach at -2.9° . Within this range of FPAs the descent CAS is held at 290 knots. This apparent change of slope is specific to the Cruise-Equals-Descent speed mode of EDA, which may speed up the aircraft in cruise in order to meet time. Since the fuel burn rate is very sensitive to the speed in cruise, rapid change of fuel burn is observed among trajectories that have varying cruise speeds. The same analysis was performed using the Descent-Only speed mode of EDA, which varies only the descent speed in order to meet the time. The resulting fuel burn change with FPA showed more “homogeneous” curves without distinct regions of different behaviors.

5 Comparison of Three Descent Strategies

Three strategies are proposed to determine the fixed FPA for EDA advisories at run time. Their advantages and disadvantages are discussed in Section 5.4. The three strategies are

1. Universally fixed FPA
2. FPA as a function of descent speed

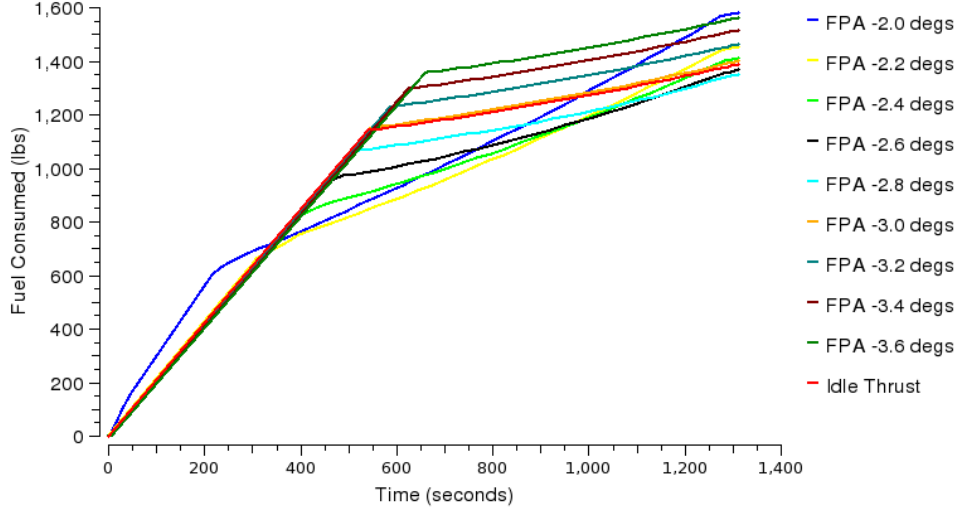


Figure 7. Accumulated fuel burn as a function of fly time. The total path distance is 150 nmi.

3. Custom FPA for every clearance

Strategy 1 issues advisories to all flights coming through a specific meter fix based on a universally fixed FPA akin to a glide slope for an Instrument Landing System (ILS). Strategy 1 is inspired by the early work of Izumi et al. [11]. Tong et al. also explored implementation of a procedure using universally fixed-FPAs for all arrival flights. When this strategy is applied, EDA fixes this FPA and iterates the speeds in order to find the meet-time trajectory for a specific arrival flight.

Strategy 2 defines the FPA as a function of the descent CAS issued in the advisory and is motivated by the descent-CAS-dependent FPA function used in the flight test in Denver Center in 2010, as shown in Table 1. Participating Skywest pilots determined the value of FPA to fly by referencing the look-up table using the descent CAS issued in the EDA clearance. The FPA function for

Table 1. The FPA function used for Skywest flights in the flight test conducted at Denver Center in 2010.

Range of Descent CAS (knots)	FPA(°)
250-260	-2.8
270-280	-3.1
290-300	-3.4
310-320	-3.8

Strategy 2 is arbitrary, although in practice it should stay in the fuel-efficient and flyable region of the descent CAS-FPA space. Considering the fact that steeper FPAs are preferred for faster descent speeds, we choose a parametric family of simple, step-wise functions of this form:

$$\gamma_i = -0.1 * \text{floor} \left(\frac{\text{DCAS} - 245}{10} \right) + \gamma_i^0, \quad (1)$$

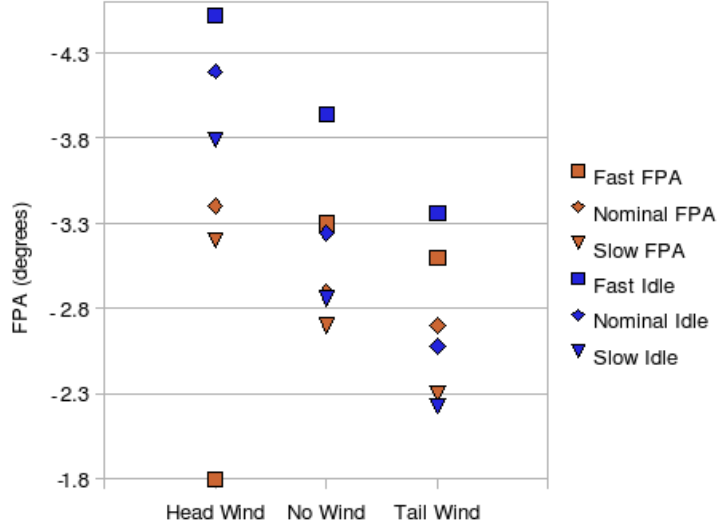


Figure 8. The fuel-optimal FPA of the fixed-FPA trajectories and the effective FPA for the corresponding idle-thrust trajectories.

where γ_i is in degrees, DCAS is the descent CAS in knots, and the parameter γ_i^0 is in degrees. Here the “floor” function returns the maximum integer that is no greater than its argument. The parameter γ_i^0 represents the value of γ_i^0 at 250 knots of descent CAS. Later analysis results in Sec. 5.4.1 justify the adequacy of this family of functions. When Strategy 2 is applied, EDA computes a set of meet-time trajectories and identify a trajectory that has a descent CAS-FPA relationship described by the FPA function. Section 5.2 discusses in detail how this is done. Both strategies 1 and 2 could presumably be published in the airport’s arrival procedures.

Strategy 3 issues a custom FPA as part of the advisory to adapt the FPA to weather, wind, and time to fly. For each arrival flight, EDA computes a set of fixed FPA, meet-time trajectories that satisfy the speed brake condition and picks the fuel-optimal trajectory as its advisory. Strategy 3 contains no parameters for optimization, but requires EDA to analyze the family of candidate meet-time trajectories in real time. Also, the FPA must be communicated explicitly between the ground and pilots.

5.1 Speed Brake Conditions

While efficiency in the model can be measured approximately by the fuel burn of the constant time-to-fly trajectory, flyability and robustness are difficult to quantify. For simplicity, we define flyability and robustness as the ability to maintain the aircraft on the desired trajectory upon uncertainty. Here uncertainty can come from errors in the predicted wind, weather, and pilots’ execution. A robust procedure should also take into account controllers’ interruptions. In all cases, power adjustment is preferred to speed brake deployment for reasons mentioned in Section 1. Since speed brake usage may still be acceptable for some aircraft types, the approach here is to compare strategies under varying degrees of acceptable speed brake usage.

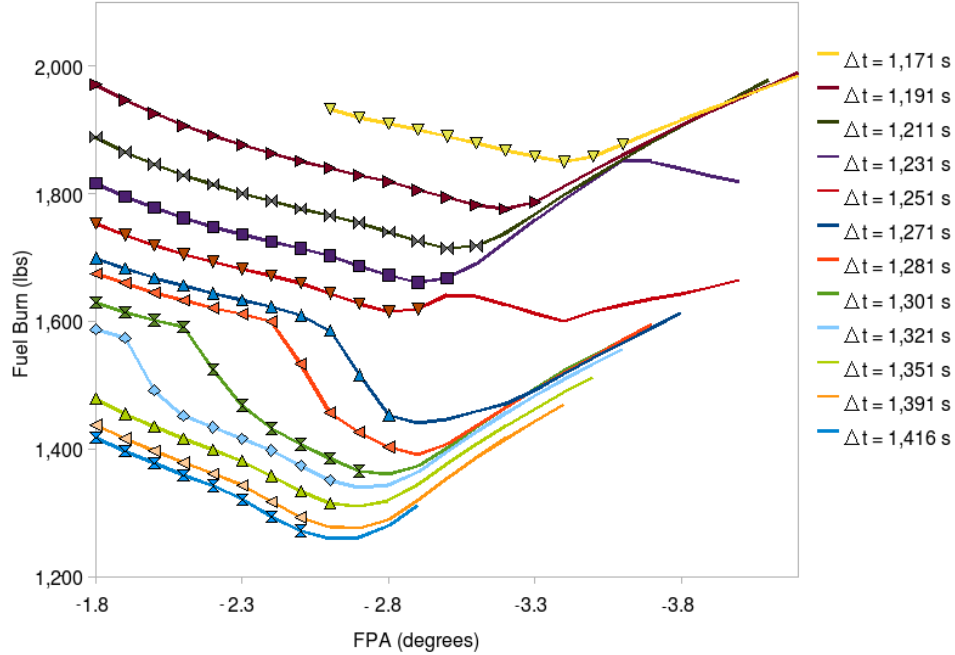


Figure 9. Fuel burn as a function of FPA and time to fly. No wind is applied. The symbols represent speed-brake-free trajectories.

For each strategy, one of three speed brake conditions is used to determine the set of feasible meet-time trajectories.

1. Any speed brake usage (SBANY) is allowed to maintain the descent FPA, as long as the speed brake usage is within the speed brake capacity defined in Section 3.2.
2. No more than 20% of the speed brake capacity (SB20) is allowed at any point during the descent.
3. No speed brake usage (SB0) is allowed during the descent.

For Strategy 3, multiple trajectories can satisfy the speed brake condition. In this case, the trajectory with the least fuel burn is selected. Note that these conditions are imposed on the analysis. Actual speed brake usage required in flight would vary based on the difference between the actual and the predicted state of the flight and atmosphere.

5.2 Parameterization of Strategies

Both strategies 1 and 2 have parameters that need to be optimized for the operational conditions. The choice of the universal fixed FPA from Strategy 1, and the FPA as a function of descent CAS for Strategy 2, are key decisions that will strongly impact the efficiency, flyability and robustness of the arrival operations.

Figure 10 illustrates how strategies 1 and 2 can select different trajectories from a set of meet-time trajectories. The value of the universal FPA parameterizes Strategy 1 and has the effect of shifting the selection line left and right on the descent CAS vs. FPA plot, as shown in Figure 10. A typical set of meet-time trajectories labeled “Trajectories 1” is shown in Figure 10, in which each square represents a trajectory’s values of descent CAS and FPA. The trajectories must all satisfy the speed brake condition of interest. The trajectory that lies on the vertical line representing strategy 1 is selected as the EDA advisory. If no meet-time trajectory is found, that particular time to fly is considered impossible to achieve based on the strategy and flight conditions.

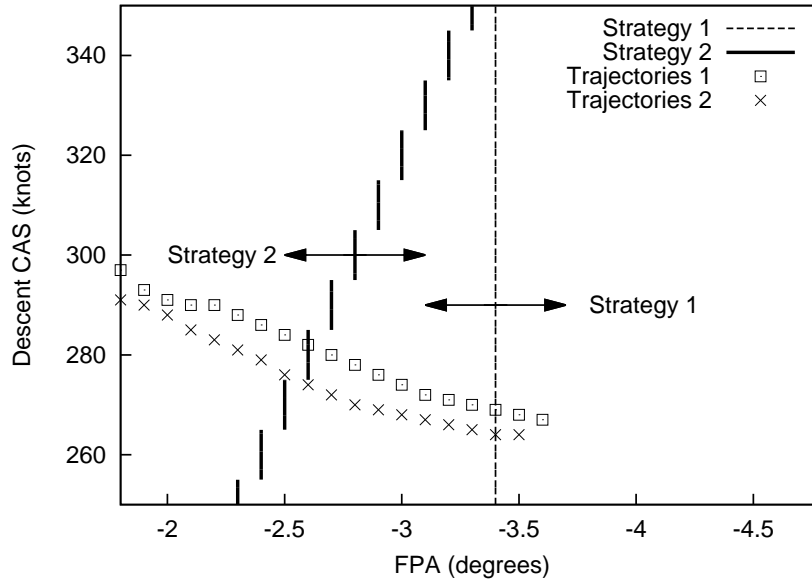


Figure 10. Demonstrating how a trajectory is selected using strategies 1 and 2 for a specific time to fly.

Strategy 2 selects from the set of meet-time trajectories the one that has a descent CAS-FPA pair that satisfies its FPA function. As shown in Figure 10, this family of functions yields shallower FPA for lower descent CAS. For a set of meet-time trajectories, the one trajectory that intercepts with this function is selected as the EDA advisory. The trajectory must also satisfy any additional speed brake condition such as SB20 or SB0. Otherwise, that particular time to fly is considered impossible to achieve based on the strategy and flight conditions. The trajectories labeled “Trajectories 2” in Figure 10 can occur during the sampling of the test conditions, in which no trajectory falls right on the vertical lines defining strategy 2. This condition will be discussed in more detail in section 5.4.1 and treated approximately in the statistics.

5.3 Sampling of Test Conditions

We consider an experiment in which EDA advisories are issued to many arrival aircraft over a wide variety of test conditions. Among the factors defining the test conditions are the variation of wind, aircraft weight, and the amount of time to delay from the nominal arrival time. For each test

condition, TS computes a set of meet-time trajectories for each strategy and accumulates statistics.

Wind is modeled as a linear function of altitude. The actual distribution of the wind strongly depends on the location and time of the year. Also, the direction of wind is far from random. Considering a generic arrival route, a random direction of the wind is sampled using a 2-D normal distribution. To estimate the width of the normal distribution, we turned to the Rapid Update Cycle (RUC) 2-hour weather prediction [25] for realistic wind distribution. We estimated the root-mean-square value of the wind speed at 35,000 ft using (RUC) 2-hour weather predictions for Denver Center from Oct. 25 to Nov. 10 in 2010. These dates were chosen because complete data sets were available and flight tests were being conducted during that time. Nine horizontal locations in the Denver Center airspace were chosen for sampling the wind predictions in RUC data. The minimum distance between any two locations is 100 nmi. The root-mean-square value was found to be 61 knots. Analysis of the RUC data for Fort Worth Center from Sep. 18 to Sep. 23 of 2011 yields a much smaller root-mean-square value of 35 knots. For the simulation, the magnitude of the wind at 35,000 ft is sampled from a normal distribution with a standard deviation of 40 knots in both X and Y directions. The standard deviation is chosen to yield a root-mean-square wind magnitude of 57 knots, a value close to but below the value of Denver Center. Since the variation of wind along a specific route may be smaller than the variation of wind averaged over locations of a Center, the choice of magnitude may qualify as an upper bound of the actual wind variation. A systematic analysis of wind data is required to support this claim.

The weight of the aircraft is sampled with a standard deviation of 8,400 lbs and a mean of 170,000 lbs. These values are estimated from the distribution of landing weights of thousands of arrival flights of this aircraft type.

Although TMA can speed up the arrival aircraft, in actual operations TMA almost always delays the aircraft. Therefore in most of this work, we sample the target time uniformly between the nominal time and the slow limit, unless noted otherwise. EDA issues a speed advisory when the delay time to absorb is small, usually less than four minutes [3]. The maximum delay time is determined by the difference in meter-fix crossing times between a trajectory flying nominal speeds and a trajectory flying minimum speeds. Note that EDA issues a clearance only when the difference between ETA and STA is greater than about 15-30 seconds. This tolerance is related to the meter flow rate specified by TMA. For this analysis we neglect this small tolerance and allow the target time to be sampled uniformly between the nominal time and the slow time.

When the target time is near the slow end of the range, the steepest trajectory could be flying at the slowest speeds flyable in the aircraft's performance model. Trajectories with steeper descents may still satisfy the speed brake condition, but they are rejected by the program because they do not absorb enough of the delay. In actual operation such descents can be made to meet the target time with path stretches. Therefore in this case, we attempt steeper descents using the slowest speeds until the descent exceeds speed brake capacity. Conceptual path stretches are added to these trajectories in order to meet the time. These path stretches are "conceptual" because we add them just to meet the time and calculate the fuel burn. We do not need to define the turn out and turn back points for them. Assuming a conceptual path stretch before the top of descent, we add to each trajectory an amount of fuel burn equal to the cruise fuel burn rate multiplied by the delay time to absorb.

5.4 Results

We conducted a Monte Carlo simulation that sampled 50,000 test conditions that varied in wind, weight, and targeted time-to-fly to the meter fix. The statistics accumulated in the simulation are used to optimize Strategy 1 and Strategy 2, and therefore enable comparison of the three strategies. For each test condition, a set of trajectories with their values of FPA ranging from -1.8° to -6.0° are computed by TS. One of three speed brake conditions was applied to the set of meet-time trajectories to reject steep descents that do not meet the speed brake condition. For each trajectory, five to ten iterations over the speeds were required to converge the solution to within the criterion of time, which is chosen to be 0.5 second. Data were accumulated during the simulation and statistics calculated. After sampling 5,000 test conditions, the statistics stabilized and did not show noticeable change.

The three fixed-FPA descent strategies defined in section 5 were applied to select a trajectory from the set of trajectories. Up to nine distinct selections can be made for each test condition as a result of the three strategies and three speed brake conditions. Strategy 3, the custom FPA approach, selects a fuel-optimal trajectory for each one of the three speed brake conditions. Strategies 1 and 2, however, have parameters that need to be determined. To determine the parameters for these two strategies, the results of applying these two parametrized strategies are stored in the simulation and analyzed for optimization.

5.4.1 Optimizing Strategies

Strategies 1 and 2 should choose parameters so that the selected advisories are close to the fuel-optimal fixed-FPA descent. On the other hand, if speed brake is utilized to a great extent in the fuel-optimal fixed FPA descent, it may be desirable to pick a shallower fixed-FPA trajectory to reduce speed brake usage, albeit at the sacrifice of certain fuel efficiency. Both factors should be considered in optimizing the parameters of the strategies with a certain level of trade-offs.

We define the fuel-burn penalty of the selected trajectory as the extra fuel burn this trajectory incurs relative to the fuel-optimal fixed-FPA trajectory computed in the same test condition. The selected trajectory should satisfy the speed brake condition of interest. The fuel-optimal fixed-FPA trajectory is chosen using SBANY. For example, the selection of any trajectory other than the $\gamma_i = -2.7^\circ$ trajectory, as shown in Figure 2, has a positive fuel-burn penalty.

Results of a Monte Carlo simulation are used to identify the preferred solution space that satisfies both low fuel burn and low speed brake. This simulation samples both fast and slow target times. Figure 11 shows the fuel burn penalty as a function of FPA and descent CAS resulting from a Monte Carlo simulation of 50,000 test conditions. The SBANY condition is applied in choosing the trajectories. Since most of the reference fuel-optimal trajectories utilize very little speed brake, as shown later in Section 5.4.2, the choice of a speed brake condition does not change the average fuel burn penalty by more than 5 lbs. A stricter speed brake condition, however, rejects steeper descents and therefore results in reduced or even empty samples in the area of high speed brake usage. All meet-time trajectories for each test condition are included in the statistics. Since each set of trajectories covers a different range of FPA and a different range of descent CAS, each descent CAS-FPA pair in the map is sampled with unequal frequencies. Roughly speaking, the low

fuel penalty, dark-blue area that spans from about -2.5° near 250 knots descent CAS to -3.5° near 350 knots descent CAS was sampled with highest frequencies. Strategies 1 and 2 should be parametrized to sample descent CAS-FPA pairs in this dark blue “valley” in order to minimize fuel burn penalty.

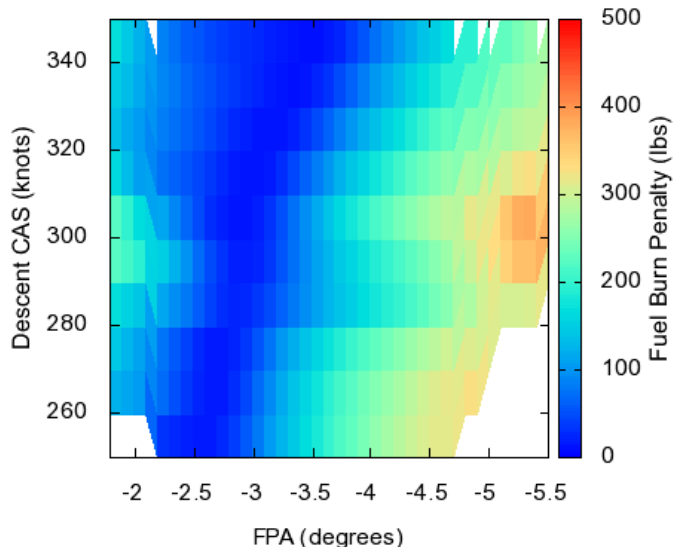


Figure 11. Fuel burn penalty averaged over 50,000 test conditions.

Figure 12 shows the speed brake usage as a function of FPA and descent CAS averaged from the same Monte Carlo simulation used for Figure 11. The speed brake usage is defined as the maximum fraction of speed brake drag coefficient relative to the speed brake capacity along the descent. The SBANY condition is applied in choosing the trajectories for comparison. Selection of the universal FPA for Strategy 1 and the FPA function for Strategy 2 should stay in the low speed brake usage region, denoted by dark blue colors.

The choice of a universal FPA for Strategy 1 and FPA function for Strategy 2 should also consider the probability of failure. If the speed brake usage of a selected trajectory exceeds the maximum allowable speed brake defined by a speed brake condition, this trajectory is rejected and the strategy fails to create an advisory in this test condition. A stringent tolerance of failure can make the procedure more robust but would be less fuel-efficient. For the purpose of this analysis, the tolerance of failure is chosen to be 1% for both strategies. In other words, if during the Monte Carlo analysis for a specific strategy, more than 1% of the conditions sampled failed to yield a trajectory, then the parameter used for this strategy is considered unacceptable. Since both Strategy 1 and Strategy 2 have one parameter each, the failure rate can be plotted as a function of this parameter.

To determine the optimal universal FPA for Strategy 1, we performed a Monte Carlo simulation that samples only the slow end of the target time, i.e., the time between nominal and slow. Figure 13 shows the resulting average fuel burn penalty and speed brake usage as a function of the universal FPA. The FPA that yields the least average fuel burn penalty is $\gamma_i = -2.7^\circ$. Since the probability of failure at $\gamma_i = -2.7^\circ$ is less than 1%, this FPA is acceptable under the SBANY condition. However at $\gamma_i = -2.7^\circ$, 24% of trajectories require speed brake usage between 0% and 20%, 14%

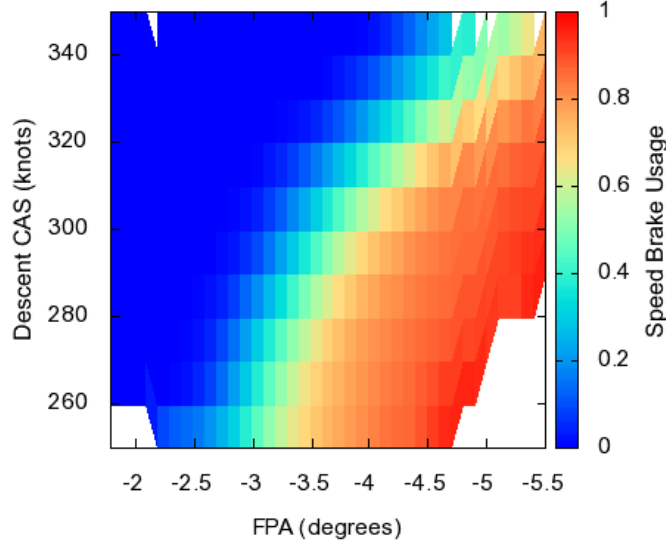


Figure 12. speed brake usage averaged over 50,000 test conditions.

of trajectories require speed brake usage between 20% and 40%, 5% of trajectories require speed brake usage between 40% and 60%, and 1% of trajectories require speed brake usage between 60% and 80%. Therefore, 20% and 44% of the trajectories at -2.7° do not satisfy the SB20 and SB0 conditions, respectively. These high probabilities of failure are unacceptable for SB20 and SB0, and shallower FPAs must be chosen such that the failure rate goes below 1%. The resulting optimal universal FPAs when imposing SB20 and SB0 are -2.3° and -2.2° , respectively.

To determine the optimal FPA function defined in Eq. 1 for Strategy 2, results of the same Monte Carlo simulation are used. Figure 14 shows the average fuel burn penalty and speed brake usage vs. the choice of the FPA function. The optimal FPA function for SBANY is

$$\gamma_i = -0.1 * \text{floor} \left(\frac{\text{DCAS} - 245}{10} \right) - 2.5^\circ, \quad (2)$$

where a value of -2.5° is assigned to the γ_i^0 in Eq. 1. Shallower values of γ_i^0 must be used for more stringent speed brake conditions to keep the probability of failure under 1%. Therefore, the optimal FPA function for SB20 is

$$\gamma_i = -0.1 * \text{floor} \left(\frac{\text{DCAS} - 245}{10} \right) - 2.2^\circ, \quad (3)$$

and the the FPA function for SB0 is

$$\gamma_i = -0.1 * \text{floor} \left(\frac{\text{DCAS} - 245}{10} \right) - 2.0^\circ. \quad (4)$$

During the simulation a small fraction of the test conditions resulted in meet-time trajectories that cross over one of the “gaps” of the FPA function without intercepting with any of the vertical segments. An example is shown in “Trajectories 2” of Figure 10. This is because the step-wise FPA

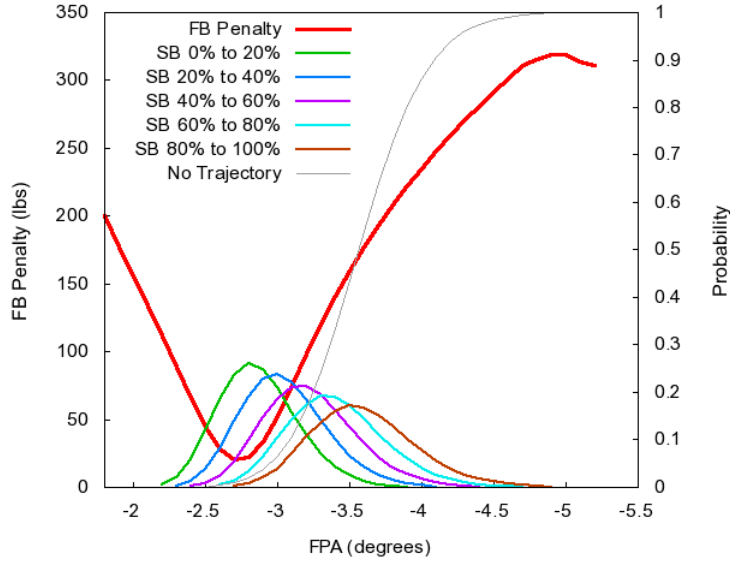


Figure 13. Fuel burn penalty and speed brake usage for Strategy 1.

function leaves gaps of three to seven seconds in the range of target time with its discrete values of FPA. Since the typical tolerance of time for EDA is 15-30 seconds [3], such gaps should cause no problem in delivering aircraft to the meter fix within the tolerance. In this case an approximate trajectory is defined by selecting the FPA in which the difference between the trajectory and function in descent CAS is the smallest. The fuel burn and speed brake usage are interpolated from the two closest trajectories using the target time.

Although the solution space of trajectories near the latest arrival time are slightly expanded to steeper FPAs by the introduction of the conceptual path stretch in Section 5.3, we find very little contribution from these trajectories in Figure 13 and Figure 14.

5.4.2 Fuel-Burn Benefits

Table 2 summarizes the fuel burn penalty for the three descent strategies under the three speed brake conditions. Again, the results are from the Monte Carlo simulation that produced Figure 13 and Figure 14. Note that all the values of fuel burn penalty are relative to the fuel-optimal fixed-FPA trajectory, which is selected with SBANY. Also, note that the values of the fuel burn penalty for strategies 1 and 2 are observed in the fuel burn penalty curves of figures 13 and 14, respectively. For each speed brake condition, Strategy 1 consumes more fuel than Strategy 2, while Strategy 2 consumes more fuel than Strategy 3. For all strategies, more stringent speed brake conditions lead to an increase of the fuel burn penalty. Compared to the SBANY condition, the SB20 condition results in extra fuel burn of 69 lbs and 34 lbs in strategies 1 and 2, respectively. The most stringent SB0 condition creates about 23 lbs and 41 lbs of extra fuel penalty than SB20 for Strategy 1 and Strategy 2, respectively. Also, shallower FPAs are selected under more stringent speed brake conditions, resulting in more fuel burn. This shift to a shallower FPA is required to accommodate the trajectories at the slow end, which required speed brake usage even for very shallow FPAs shown

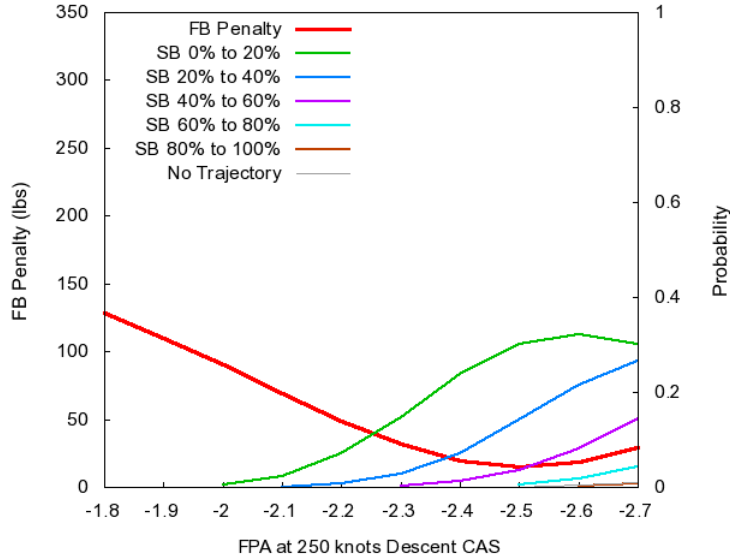


Figure 14. Fuel burn penalty, probability of speed brake usage, and failure rate for different FPA functions used for Strategy 2. The X-axis FPA represents the intercept of the function with 250 knots descent CAS, the value of γ_i^0 in Eq. 1.

in the bottom part of Figure 12. The custom FPA strategy, denoted as Strategy 3 in Section 5, is relatively insensitive to the speed brake condition, as the fuel burn penalty relative to SBANY goes up to only 5 lbs for SB0. This implies that most of the fuel-optimal fixed-FPA descents for the test conditions sampled utilize very little speed brake.

Table 2. The fuel burn penalty for the three strategies under the three speed brake conditions averaged over 50,000 test conditions.

Strategy\Fuel burn penalty (lbs) and FPA($^{\circ}$)	Speed Brake Condition		
	Any	$\leq 20\%$	None
Strategy 1, Universal FPA	20	89	112
FPA	-2.7	-2.3	-2.2
Strategy 2, Descent CAS function	15	49	90
FPA at 250 knots(γ_i^0)	-2.5	-2.2	-2.0
Strategy 3, Custom FPA	0	0.1	5
Idle		41	

Section 4.1 demonstrated that, in one test condition observed in Figure 2, fixed-FPA trajectories can be more fuel-efficient than the idle-thrust descent. The bottom row of Table 2 shows that, of all the sampled test conditions, a custom FPA strategy with SBANY can save 41 lbs of fuel relative to the idle-thrust descents on average. This should not be surprising. The results of Izumi et al. for Boeing 747 showed fuel-optimal descent trajectory burns 50 to 60 lbs less than the idle-

thrust descent [12]. It is possible that, on average of the test conditions, a fuel-optimal fixed-FPA trajectory for this aircraft type is closer to the fuel-optimal trajectory than the idle-thrust descent is, resulting in the average fuel burn benefit.

6 Discussion

The cruise and descent speeds computed in both Section 4 and Section 5 are considered continuous. In actual operations, the cruise and descend speeds issued in an EDA clearance may consider the precision of the equipment of the aircraft. For some small aircraft, the CAS values may need to be constrained to increments of 10 knots. The latest human-in-the-simulation of EDA attempts to model this limitation (unpublished). The effect of such limitations on the accuracy of the delivered meet time remains to be investigated. We believe the descent strategies should be able to accommodate these limitations.

Figure 6 of Section 4.1 shows that the fuel burn rate is very sensitive to an increase in cruise speed. This can hardly be desirable in practice except for the purpose of conflict resolution. If EDA needs to speed up an aircraft, we believe it should increase the descent speed first. Only when the descent speed cannot be fast enough to meet the target time should EDA speed up the aircraft in cruise. Similarly, EDA should decrease the cruise speed before decreasing the descent speed to slow down the aircraft. The current Cruise-And-Descent mode can potentially be modified to adopt this behavior.

The aircraft's preferred descent speed was modeled as 290 knots in this work. This choice defines the nominal trajectory and the nominal time-to-fly. In practice this speed is not only determined by the aircraft type but also by the airline. For Section 5, another Monte Carlo simulation using 300 knots as the nominal descent was conducted, and the results showed that this choice of speed had only minor effects on the statistics in Table 2.

Figure 12 of Section 5.4.1 shows that speed brake usage occurs even for very shallow FPAs in the low descent CAS region. This is due to the fact that strong tail winds prevail in the statistics for this region. Therefore, speed brakes are used to great extent to compensate for the tail wind. The high speed brake usage of these test conditions shifts the optimal FPAs in strategies 1 and 2 towards shallower FPAs for the SB20 and SB0 conditions. This shift tends to increase the average fuel burn penalty of the strategy. A possible improvement of the fuel-burn benefit of a strategy is to treat trajectories near the slow end with a different FPA function that uses shallower FPAs. The original FPA function, be it a universal fixed FPA or a function given in Eq. 1, can be combined with this second FPA function at the 265 knots descent CAS boundary.

Table 2 of Section 5.4.2 shows that Strategy 1 and Strategy 2 lead to more fuel burn than Strategy 3, especially for stricter speed brake conditions. Strategy 1 and Strategy 2 do not require FPA to be communicated to the aircraft and can presumably be published in the arrival procedures. Strategy 1 is slightly simpler to implement than strategy 2, and may result in fewer pilot execution errors. Although Strategy 3 provides most fuel-efficient descent profile, it requires FPA to be communicated to the pilot before top-of-descent via voice or data-link.

Table 2 also shows that, for a meet-time constraint, fixed-FPA descents can burn less fuel than idle-

thrust descents when averaged over the test conditions. However, individual test conditions may favor either the fixed-FPA descent or the idle-thrust descent. Section 4.1 investigated the fuel burn and speed brake usage for a specific test condition. The results showed 38 lbs fuel benefits of the fuel-optimal fixed-FPA trajectory over the idle-thrust trajectory. Limited amount of analysis under different test conditions revealed that such fuel benefit is greatest in a head wind and diminishes in a tail wind. In fact, with a strong tail wind the idle-thrust trajectory seems to always have fuel burn benefits. In this case the idle-thrust trajectory has an earlier top-of-descent than the fuel-optimal fixed-FPA trajectory in the tail wind condition. More analysis is needed to provide a systematic description of wind effects on the competition of a fuel-optimal fixed-FPA trajectory and an idle-thrust trajectory. In addition to fixed-FPA descents, other types of low-power descents can potentially also be more fuel-efficient than idle-thrust descents. It would be interesting to see if similar fuel benefits can be observed in smaller aircraft types such as business or regional jets.

The optimal parameters for strategies 1 and 2 will vary for every specific arrival route. The prevailing wind along each arrival route has a major influence in the optimization of these parameters. The wind variation sampled in the simulation has complete random directions, and we believe the choice of wind distribution may be somewhat larger than a typical wind variation along a specific arrival route. This remains to be confirmed. When strategies 1 and 2 are customized for an arrival route, the smaller variation of wind may lead to less fuel burn penalties. However, variation of performance among aircraft types has not been modeled, and is expected to increase the fuel burn penalty for strategies 1 and 2. The effects of these factors remain to be investigated.

7 Conclusion

This work modelled fixed-flight-path-angle (fixed-FPA) descents, performed sensitivity analysis of the input parameters, and compared three FPA selection strategies that were applied to realistic test conditions for the En-route Descent Advisor (EDA). A high-fidelity performance model of a mid-size twin-engine jet was chosen from the aircraft performance database of the Center-TRACON Automation System for computing trajectories.

The first part of this work studied in depth the sensitivity of fuel burn and speed brake usage to FPA for a typical operational condition. Sensitivity of the fuel-optimal FPA to winds and target times was also investigated.

The second part of this work proposed three FPA selection strategies given below:

1. Universally fixed FPA
2. FPA as a function of descent speed
3. Custom FPA for every clearance.

The sensitivity of fuel burn to the selection strategies and speed brake usage was studied. To take into account robustness requirements in the optimization of the FPA selection strategies, three speed brake conditions were imposed on the selection of the FPA:

1. Any speed brake usage (SBANY) is allowed to maintain the descent FPA, as long as the speed brake usage is within the speed brake capacity.
2. No more than 20% of the speed brake capacity (SB20) is allowed at any point during the descent.
3. No speed brake usage (SB0) is allowed during the descent.

Monte Carlo simulations were performed to sample 50,000 realistic test conditions. The results showed that Strategy 1 and Strategy 2 burn more fuel than Strategy 3. Strategy 3 was the most fuel-efficient, but requires explicit communication of the FPA between the ground and the pilot prior to the top-of-descent. Stringent speed brake conditions, although they may increase robustness of the procedure, do reduce the fuel efficiency of the procedures. Strategy 1 and Strategy 2 were more sensitive to speed brake conditions and can have up to 112 lbs and 90 lbs of fuel burn penalty when speed brake usage was disallowed.

Contrary to some literature that referred to an idle-thrust descent as a fuel-optimal descent, results of this work showed that idle-thrust descents burned 41 lbs more fuel than the fuel-optimal fixed-FPA descents on average of the test conditions sampled. In some test conditions particularly head-wind and no-wind, fuel can be saved by a top-of-descent earlier than that of an idle-thrust descent. The extra fuel burn arising from the inefficient descent segment is more than compensated by the reduced fuel burn in the cruise segment.

Our next steps are to analyze other aircraft types to understand sensitivity/variation of the optimal FPA for descent in aircraft types. We also plan to develop adequate models for typical RJ/BJ types. The Base of Aircraft Data (BADA) [26] may provide a good starting point for such models. Another future direction is to include path stretches and step-downs in our fuel-burn analysis.

Acknowledgments

We thank Richard Copenbarger and David Williams for helpful discussions.

References

1. Nagle, G.; Sweet, D.; Carr, G.; Felipe, V.; Trapani, A.; Copenbarger, R.; and Hayashi, M.: Human-in-the-Loop Simulation of the Efficient Descent Advisor for 3D Path Arrival Management. *Proceedings of the AIAA Aircraft Technology, Integration, and Operations Conference*, AIAA-2011-6877, Virginia Beach, VA, 2011.
2. Copenbarger, R.; Dyer, G.; Hayashi, M.; Lanier, R.; Stell, L.; and Sweet, D.: Development and Testing of Automation for Efficient Arrivals in Constrained Airspace. *Proceedings of the 27th International Congress of the Aeronautical Sciences*, ICAS2010-11.11.3, Nice, France, 2010.
3. Copenbarger, R. A.; Lanier, R.; Sweet, D.; and Dorsky, S.: Design and Development of the En Route Descent Advisor (EDA) for Conflict-Free Arrival Metering. *Proceedings of the AIAA Guidance, Navigation, and Control Conference*, AIAA-2004-4875, Aug. 2004.

4. Mueller, K. T.; Schleicher, D. R.; and Coppenbarger, R. A.: Improved Aircraft Path Stretch Algorithms for the En Route Descent Advisor (EDA). *Proceedings of the AIAA Guidance, Navigation, and Control Conference*, AIAA-2003-5571, Aug. 2003.
5. Green, S. M.; and Vivona, R. A.: En Route Descent Advisor Concept for Arrival Metering. *Proceedings of the AIAA Guidance, Navigation, and Control Conference*, AIAA-2001-4114, Aug. 2001.
6. Federal Aviation Administration, FAA's NextGen Implementation Plan. Mar. 2011.
7. Isaacson, D. R.; Robinson, J. E.; Swenson, H.; and Genery, D. G.: A Concept for Robust, High Density Terminal Air Traffic Operations. *Proceedings of the 10th AIAA Aviation Technology, Integration, and Operations Conference*, AIAA-2010-9292, Sept. 2010.
8. Erzberger, H.: Transforming the NAS: The Next Generation Air Traffic Control System. *Proceedings of the 24th International Congress of the Aeronautical Sciences*, ICAS 2004-8.1.2 (I.L.), Aug. 2004.
9. Swenson, H. N.; Hoang, T.; Engelland, S.; Vincent, D.; Sanders, T.; Sanford, B.; and Heere, K.: Design and Operational Evaluation of the Traffic Management Advisor at the Fort Worth Air Route Traffic Control Center. *Proceedings of the 1st USA/Europe Air Traffic Management R&D Seminar*, June 1997.
10. Tong, K.-O.; Schoemig, E.; Boyle, D.; Scharl, J.; and Haraldsdottir, A.: Descent Profile Options for Continuous Descent Arrival Procedures within 3d Path Concept. *Proceedings of the IEEE/AIAA 26th Digital Avionics Systems Conference*, Oct. 2007, pp. 3.A.3-1 – 3.A.3-11.
11. Izumi, K. H.: Sensitivity Studies of 4D Descent Strategies in an Advanced Metering Environment. *Proceedings of the American Control Conference, 1986*, June 1986, pp. 687-692.
12. Izumi, K. H.; Schwab, R. W.; Groce, J. L.; and Coote, A.: An Evaluation of Descent Strategies for TNAV-Equipped Aircraft in an Advanced Metering Environment ATOPS. NASA CR-178093, Boeing Commercial Airplane Company, Dec. 1986.
13. Williams, D. H.: Impact of Mismodeled Idle Engine Performance on Calculation and Tracking of Optimal 4-D Descent Trajectories. *Proceedings of the 5th American Control Conference*, vol. 2, 1986, pp. 681-686.
14. Williams, D. H.; and Green, S. M.: Flight Evaluation of Center-TRACON Automation System Trajectory Prediction Process. NASA/TP-1998-208439, July 1998.
15. Stell, L.: Analysis of Flight Management System Predictions of Idle-thrust Descents. *Proceedings of the IEEE/AIAA 29th Digital Avionics Systems Conference*, Oct. 2010.
16. Stell, L.: Prediction of Top of Descent Location for Idle-thrust Descents. *Proceedings of the 9th USA/Europe Air Traffic Management R&D Seminar*, June 2011.
17. Weidner, T.; Davidson, T. G.; and Birtcil, L.: Potential Benefits of User-Preferred Descent Speed Profile. NASS AATT TO26 Seagull TR98188.26-02, Seagull Technologies, Dec. 2000.

18. Shrestha, S.; Neskovic, D.; and Williams, S. S.: Analysis of Continuous Descent Benefits and Impacts During Daytime Operation. *Proceedings of the 8th USA/Europe Air Traffic Management R&D Seminar*, June 2009.
19. Landry, S.; Farley, T.; Foster, J.; Green, S.; Hoang, T.; and Wong, G. L.: Distributed scheduling architecture for multi-center time-based metering. *Proceedings of the AIAA Aviation Technology, Integration, and Operations Conference*, AIAA-2003-6758, Nov. 2003.
20. Slattery, R.; and Zhao, Y.: En-route Descent Trajectory Synthesis for Air Traffic Control Automation. *Proceedings of the American Control Conference*, vol. 5, June 1995, pp. 3430–3434.
21. Slattery, R.; and Zhao, Y.: Trajectory Synthesis for Air Traffic Automation. *Journal of Guidance, Control and Dynamics*, vol. 20, no. 2, Mar. 1997, pp. 232–238.
22. Lee, A. G.; Bouyssounouse, X.; and Murphy, J. R.: The Trajectory Synthesizer Generalized Profile Interface. *Proceedings of the 10th AIAA Aviation Technology, Integration, and Operations Conference*, AIAA-2010-9138, Sept. 2010.
23. Gong, C.; and Chan, W. N.: Using Flight Manual Data to Derive Aero-propulsive Models for Predicting Aircraft Trajectories. *Proceedings of the AIAA Aircraft Technology, Integration, and Operations Conference*, AIAA-2002-5844, Oct. 2002.
24. Peixoto, J. P.; and Oort, A. H.: *Physics of Climate*, American Institute of Physics. 1992, pp. 154–155.
25. Benjamin, S. G.; Brown, J. M.; Brundage, K. J.; Schwartz, B.; Smirnova, T.; Smith, T. L.; Morone, L. L.; and Dimego, G.: The Operational RUC-2. Preprints. *Proceedings of the 16th Conference on Weather Analysis and Forecasting*, Amer. Meteor. Soc., 1998, pp. 249–252.
26. Nuic, A.; Poinot, C.; Iagaru, M.-G.; Gallo, E.; Navarro, F. A.; and Querejeta, C.: Advanced Aircraft Performance Modeling for ATM: Enhancements to the BADA Model. *Proceedings of the IEEE/AIAA 24th Digital Avionics Systems Conference*, Nov. 2005.